

-
- [65] Bounhar, Y; Zhang, Y; Goodyer, CG and LeBlanc, A. Prion protein protects human neurons against Bax-mediated apoptosis. *J Biol Chem*, 2001 276, 39145-9
- [66] Pisani, A; Bonsi, P and Calabresi, P. Calcium signaling and neuronal vulnerability to ischemia in the striatum. *Cell Calcium*, 2004 36, 277-84
- [67] Colling, SB; Collinge, J and Jefferys, JG. Hippocampal slices from prion protein null mice: disrupted Ca(2+)-activated K⁺ currents. *Neurosci Lett*, 1996 209, 49-52
- [68] Herms, JW; Korte, S; Gall, S; Schneider, I; Dunker, S and Kretzschmar, HA. Altered intracellular calcium homeostasis in cerebellar granule cells of prion protein-deficient mice. *J Neurochem*, 2000 75, 1487-92
- [69] DeArmond, SJ and Prusiner, SB. Etiology and pathogenesis of prion diseases. *Am J Pathol*, 1995 146, 785-811
- [70] Yokoyama, T; Kimura, KM; Ushiki, Y; Yamada, S; Morooka, A; Nakashiba, T; Sassa, T and Itohara, S. In vivo conversion of cellular prion protein to pathogenic isoforms, as monitored by conformation-specific antibodies. *J Biol Chem*, 2001 276, 11265-71
- [71] Kitamoto, T; Amano, N; Terao, Y; Nakazato, Y; Isshiki, T; Mizutani, T and Tateishi, J. A new inherited prion disease (PrP-P105L mutation) showing spastic paraparesis. *Ann Neurol*, 1993 34, 808-13
- [72] Neufeld, MY; Josiphov, J and Korczyn, AD. Demyelinating peripheral neuropathy in Creutzfeldt-Jakob disease. *Muscle Nerve*, 1992 15, 1234-9
- [73] Tuzi, NL; Gall, E; Melton, D and Manson, JC. Expression of doppel in the CNS of mice does not modulate transmissible spongiform encephalopathy disease. *J Gen Virol*, 2002 83, 705-11
- [74] Forloni, G; Angeretti, N; Chiesa, R; Monzani, E; Salmona, M; Bugiani, O and Tagliavini, F. Neurotoxicity of a prion protein fragment. *Nature*, 1993 362, 543-6
- [75] Chen, SG; Teplow, DB; Parchi, P; Teller, JK; Gambetti, P and Autilio-Gambetti, L. Truncated forms of the human prion protein in normal brain and in prion diseases. *J Biol Chem*, 1995 270, 19173-80

Chelating Compound, Chrysoidine, Is More Effective in Both Antiprion Activity and Brain Endothelial Permeability Than Quinacrine

Katsumi Doh-ura,^{1,5} Kazuhiko Tamura,² Yoshiharu Karube,³ Mikihiro Naito,⁴ Takashi Tsuruo,⁴ and Yasufumi Kataoka²

Received July 26, 2006; accepted September 27, 2006

SUMMARY

1. As an extension of our previous study of quinacrine and its derivatives, chelating chemicals were screened to obtain more effective, better brain-permeable antiprion compounds using either prion-infected neuroblastoma cells or brain capillary endothelial cells.

2. Eleven chemicals were found to have antiprion activity. Most of them shared a common structure consisting of benzene or naphthalene at either end of an azo bond. Structure–activity data suggest that chelating activity is not necessary but might contribute to the antiprion action.

3. Chrysoidine, a representative compound found here, was about 27 times more effective in the antiprion activity and five times more efficiently permeable through the brain capillary endothelial cells than quinacrine was.

4. These chemicals might be useful as compounds for development of therapeutics for prion diseases.

KEY WORDS: prion; chrysoidine; blood–brain barrier; aromatic azo compounds; therapy; chelating agents; brain endothelial cells; prion-infected neuroblastoma cells.

INTRODUCTION

Transmissible spongiform encephalopathies or prion diseases are fatal neurodegenerative disorders that include Creutzfeldt–Jakob disease and Gerstmann–Sträussler–Scheinker syndrome in humans, and scrapie, bovine spongiform encephalopathy, and chronic wasting disease in animals. These disorders are characterized by accumulation in the brain of an abnormal isoform of prion protein

¹Department of Prion Research, Tohoku University Graduate School of Medicine, Sendai, Japan.

²Department of Pharmaceutical Care and Health Sciences, Faculty of Pharmaceutical Sciences, Fukuoka University, Fukuoka, Japan.

³Department of Drug Design and Drug Delivery, Faculty of Pharmaceutical Sciences, Fukuoka University, Fukuoka, Japan.

⁴Institute of Molecular and Cellular Biosciences, University of Tokyo, Tokyo, Japan.

⁵To whom correspondence should be addressed at Department of Prion Research, Tohoku University Graduate School of Medicine, 2-1 Seiryō-cho, Aoba-ku, Sendai 980-8575, Japan; e-mail: doh-ura@mail.tains.tohoku.ac.jp.

(PrP), which is putatively a main component of pathogens or the pathogen itself, and which is rich in beta-sheet structure and resistant to digestion with proteinase K (Prusiner, 1991). Recent outbreaks of variant Creutzfeldt–Jakob disease and iatrogenic Creutzfeldt–Jakob disease through use of cadaveric growth hormone or dural grafts in younger people have necessitated the development of suitable therapies.

We previously found quinacrine and its derivatives to have potent antiprion activity in prion-infected cells (Doh-Ura *et al.*, 2000; Murakami-Kubo *et al.*, 2004). The common structure of these chemicals, a quinoline ring with a side chain containing a nitrogen atom located at a particular distance from another nitrogen atom in the ring indicates that the chemicals have chelating activity, but the involvement of chelating metals in their antiprion activity has never been confirmed. Quinacrine has been used recently for clinical trials of patients with prion diseases in several countries. Orally administered quinacrine is reportedly effective in transiently improving cognitive functions of patients (Nakajima *et al.*, 2004), but it frequently causes such adverse effects as liver dysfunction. For that reason, either improving its penetration into the brain (the target organ of prion diseases) or reducing its uptake into the liver is suggested for producing more beneficial results (Dohgu *et al.*, 2004).

Here, to obtain more effective antiprion compounds with better brain permeability than quinacrine, we screened chelating chemicals in prion-infected neuroblastoma cells. We investigated the brain permeability of a representative chemical using an *in-vitro* model for the blood–brain barrier.

MATERIALS AND METHODS

Chemicals and Cells

Chemicals used in the study were purchased from Sigma-Aldrich Corp. (St. Louis, MO), Tokyo Kasei Kogyo Co. Ltd. (Tokyo, Japan), and Wako Pure Chemical Industries Ltd. (Osaka, Japan). All chemicals, except for chrysoidine, were dissolved in 100% dimethyl sulfoxide (DMSO), although chrysoidine was dissolved in distilled water.

Acetylated Yellow AB was obtained as follows. Yellow AB was dissolved in dichloromethane and mixed with excess glacial acetic acid. After its complete acetylation was observed by thin layer chromatography, the acetylated product was purified using silica gel column chromatography (dichloromethane/ethyl acetic acid: 9/1 (v/v)). The residual solid was lyophilized and identified as acetylated Yellow AB by both fast atom bombardment mass spectrometry and elemental analysis.

Murine neuroblastoma (NB) cells that had been persistently infected with the scrapie prion strain RML (ScNB cells) (Race *et al.*, 1988) were used for the assay of antiprion activity and grown in Opti-MEM (Invitrogen Corp., CA) containing 10% fetal bovine serum. For the assay of brain endothelial permeability, immortalized endothelial cells from the murine brain capillary (MBEC4 cells) (Tatsuta *et al.*, 1992) were used and grown in DMEM (Invitrogen Corp., CA) containing 10% fetal bovine serum, 100 μ g/mL streptomycin, and 100 units/mL penicillin.

Antiprion Activity Assay

Antiprion activity of a chemical was assayed by measuring its 50% inhibition dose (IC_{50}) for abnormal PrP formation in ScNB cells, as described previously (Doh-Ura *et al.*, 2000; Ishikawa *et al.*, 2004). Each chemical was added at designated concentrations when cells were passed at 10% confluency. The final concentration of DMSO in the medium was maintained at less than 0.5%. The cells were allowed to grow to confluence and were lysed with a lysis buffer (0.5% sodium deoxycholate, 0.5% Nonidet P-40, PBS). The lysates were digested with 10 μ g/mL proteinase K for 30 min and centrifuged at $100,000 \times g$ for 30 min at 4°C. The pellets were resuspended in the sample loading buffer and boiled. The samples were separated using electrophoresis on a 15% Tris-glycine-SDS-polyacrylamide gel and electroblotted. Detection of PrP was done using an antibody PrP-2B, followed by an alkaline phosphatase-conjugated secondary antibody. Immunoreactive signals were visualized with CDP-Star detection reagent (GE Healthcare Bio-Science, NJ) and were analyzed densitometrically. Three independent assays were performed in each experiment.

Cellular PrP Assay

The total level of normal cellular PrP was assayed similarly in noninfected NB cells treated with a chemical. Briefly, the cells were treated with a chemical as described earlier and lysed with the lysis buffer. Four volumes of the lysate were added to one volume of the five times concentrated sample loading buffer and boiled. Then, the samples were analyzed by immunoblotting as described earlier. The cell surface level of normal cellular PrP was assayed by flow cytometry described previously (Kim *et al.*, 2004). Briefly, NB cells dispersed by the treatment with ice-cold PBS containing 0.1% collagenase (Wako Pure Chemicals, Osaka, Japan) were washed with 0.5% fetal bovine serum in PBS (FBS/PBS) and incubated with an antibody SAF83 (1:500) (SPI-BIO, Massy, France) for 30 min on ice. Cells were washed with FBS/PBS and incubated with goat F(ab')₂ fragment antimouse IgG(H + L)-PE (Beckman Coulter, CA) for 30 min. After washing, cells were analyzed using an EPICS XL-ADC flow cytometer (Beckman Coulter, CA).

Surface Plasmon Resonance Assay

Binding assay of a chemical with recombinant PrP was performed using an optical biosensor (Biacore AB, Uppsala, Sweden), as described previously (Kawatake *et al.*, 2006). Briefly, recombinant mouse PrP (amino acids 121–231; PrP121–231) was immobilized on a biosensor chip at a density of *ca.* 3,000 resonance units (RU) using amine coupling. Test chemicals were diluted to 50 μ M with the running buffer (3% DMSO in PBS, pH 7.4) and were injected over both the PrP flow cell and the reference at a flow rate of 20 μ L/min. The dissociation phase was monitored with injection of the running buffer at a flow rate of 20 μ L/min. The flow cell was washed with 10 mM NaOH for 30 s between sample injections. Buffer blanks for double referencing were injected before sample analyses.

Brain Endothelial Permeability Assay

Permeability assay was performed as described previously (Dohgu *et al.*, 2004). Briefly, MBEC4 cells were cultured on the collagen-coated polycarbonate membrane of a Transwell insert (Corning Coster Corp., MA). Before assay, the cells were washed with Krebs–Ringer buffer (118 mM NaCl, 4.7 mM KCl, 1.3 mM CaCl₂, 1.2 mM MgCl₂, 1.0 mM NaH₂PO₄, 25 mM NaHCO₃, 11 mM D-glucose, pH 7.4). Then, the buffer (1.5 mL) was added outside of the insert (abluminal side), and the buffer (0.5 mL) containing 100 μ M of a chemical was loaded on the luminal side of the insert. Samples (0.5 mL) were recovered from the abluminal chamber at 10, 20, 30, and 60 min and replaced immediately with fresh Krebs–Ringer buffer. Sodium fluorescein (Na-F, MW 376; Sigma-Aldrich Corp., MO) was used as a paracellular transport marker, and chrysoidine (Tokyo Kasei Kogyo Co. Ltd., Tokyo, Japan) as a test chemical, in addition to quinacrine as a control. The chemical concentration was measured by either determining the fluorescent intensity of Na-F (Ex(λ) 485 nm; Em(λ) 530 nm) and quinacrine (Ex(λ) 450 nm; Em(λ) 530 nm) or determining the absorbance of chrysoidine at 450 nm. The permeability coefficient was calculated using the slope of clearance curve for each chemical obtained during the 60-min period according to the method described by Dehouck *et al.* (Dehouck *et al.*, 1992). Statistical analysis was performed using one-way analysis of variance followed by Tukey–Kramer method for multiple comparisons.

RESULTS

Antiprion Screening *in vitro*

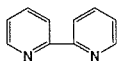
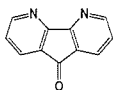
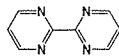
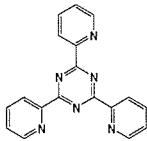
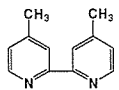
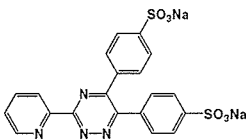
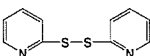
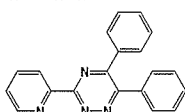
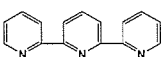
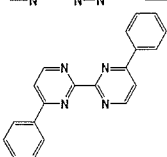
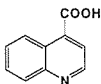
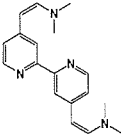
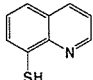
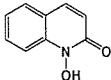
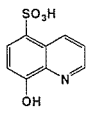
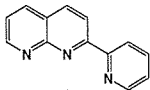
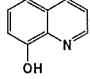
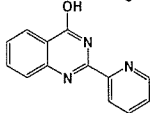
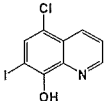
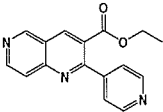
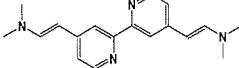
To evaluate functional groups of antiprion chelating chemicals, various chelating chemicals were examined for whether they inhibited abnormal PrP formation in prion-infected ScNB cells. Thirty-five chelating chemicals were analyzed; 11 of them were effective in inhibiting abnormal PrP formation for doses at which cell toxicity was not observed (Tables I and II). Nine of the 11 effective chemicals had a common structure, which consisted of aromatic rings (terminals 1 and 2 in Table II) at both ends of an azo bond. Although both 4-methyl-2-(2-thiazolylazo)phenol and 4-(2-pyridylazo)resorcinol were not effective, they also exhibited this structure, with a thiazole ring and a pyridine ring in the terminal 1 portion, respectively. Their lack of effectiveness might be attributable to cell toxicity, which occurred at lower doses than for chemicals carrying a benzene ring in the terminal 1 portion. On the other hand, all chemicals carrying either a benzene ring or a naphthalene ring in the terminal 2 portion were effective. Therefore, the data suggest that a structure with such an aromatic ring as benzene or naphthalene in either end of an azo bond might be responsible for inhibiting abnormal PrP formation in ScNB cells.

Mechanism of Antiprion Action

We tested whether the effective chemicals cause any alteration of the cellular PrP level in the treated cells because reduction in the cellular PrP level engenders

Aromatic Azo Chemicals with Antiprion Activity

Table I. Antiprion Activity in ScNB Cells of Chelating Compounds

Compound	IC ₅₀ (μM)	CM (μM)	Compound	IC ₅₀ (μM)	CM (μM)
	-	75		-	>100
	-	>100		-	25
	-	10		-	>100
	-	10		-	10
	-	0.5		5	25
	-	>100		-	5
	-	5		-	25
	-	>100		25	>200
	-	5		-	10
	-	10		-	>100
				-	5

Note. IC₅₀: approximate dose giving 50% inhibition of abnormal PrP formation relative to the control.
CM: approximate maximal dose that does not affect the rate of cell growth to confluence.

Table II. Antiprion Activity in ScNB Cells of Chelating Azo Compounds

Compound	Terminal 1 -N=N-	Terminal 2	IC ₅₀ (μM)	CM(μM)
Phenylazoresorcinol			0.3	50
2-Phenylazo-4-methylphenol			0.3	75
4-Methyl-2-(2-thiazolylazo)phenol			-	0.5
1-(2-Thiazolylazo)-2-naphtol			-	0.5
4-(2-Thiazolylazo)resorcinol			3	5
TAMSMB			-	>100
4-(2-Pyridylazo)resorcinol			-	0.25
1-(2-Pyridylazo)-2-naphtol			-	1
5-Br-PAPS			15	20
5-Br-PADAP			4	10
5-Cl-PADAP			2	5
5-CF ₃ -PADAP			4	10
Yellow AB			0.5	100
Chrysoidine			0.015	>100
Congo red			0.014	not tested
Quinacrine			0.4	2

Note. IC₅₀: approximate dose giving 50% inhibition of abnormal PrP formation relative to the control. CM: approximate maximal dose that does not affect the rate of cell growth to confluence. TAMSMB: 4-methyl-5-sulfomethylamino-2-(2-thiazolylazo)benzoic acid. PAPS: 2-(2-pyridylazo)-5-[*N-n*-propyl-*N*-(3-sulfopropyl)amino]phenol, disodium salt. PADAP: 2-(2-pyridylazo)-5-diethylaminophenol.

reduction in abnormal PrP formation. The results revealed no reduction in the cellular PrP level of the cells (Fig. 1(A) and (B)). Furthermore, either to examine whether the chemicals directly destabilize or denature the abnormal PrP structure or to exclude the possibility of interference with preparation and immunodetection of the abnormal PrP, the cell lysate either alone or mixed with the chemicals was incubated at 37°C for 1 h prior to proteinase K digestion; it was then processed ordinarily to obtain the abnormal PrP. The results indicated that the chemicals did not affect the abnormal PrP signals (Fig. 1(C)).

Because it was predicted that the chemicals might exert their antiprion action through a certain mechanism involving chelating metals, the most effective chemical found here, chrysoidine, was preincubated before addition to the ScNB culture medium with an equivalent dose or lower doses of various metal ions, including copper, zinc, cobalt, and aluminum ions. The results revealed no change in the inhibition activity of the chemical (Fig. 2). Furthermore, to examine whether chelating activity is necessary for antiprion action, we modified Yellow AB in such a manner that its amino base was acetylated to remove its chelating activity. The acetylated Yellow AB was tested in ScNB cells, and it was one-eighth as effective in inhibiting abnormal PrP formation as Yellow AB (Fig. 3(A)). Finally, as a chemical bearing the effective structure but lacking chelating activity, the chemical azobenzene, which is most similar in the structure to the chemical chrysoidine, was tested. It was about 30 times less effective than chrysoidine (Fig. 3(B)). These findings suggest that chelating activity is not essential for the antiprion action but might influence it.

Interaction with Recombinant PrP

We previously reported that more potent antiprion agents have higher affinity to recombinant PrP121–231 in surface plasmon resonance (SPR) analysis (Kawatake *et al.*, 2006). Therefore, we examined whether this is also demonstrated in the effective chelating chemicals found here. Six of the chemicals (each at 50 μ M) were tested. The SPR sensorgrams of the chemicals except 4-(2-pyridylazo)resorcinol showed similarly weak signal responses of less than 100 RU as quinacrine did (Fig. 4). However, neither 4-(2-thiazolylazo)resorcinol nor Yellow AB reached the equilibrium state at the association phase; neither 4-(2-thiazolylazo)resorcinol nor 2-phenylazo-4-methylphenol returned to the baseline at the dissociation phase. In contrast, 4-(2-pyridylazo)resorcinol showed the strongest response of more than 200 RU and neither reached the equilibrium state at the association phase nor returned to the baseline at the dissociation phase. The binding response value from the sensorgram (equilibrium or maximum response value divided by molecular weight), which is an index for estimating the interaction of a chemical with the molecules sited on a biosensor chip (Frostell-Karlsson *et al.*, 2000), showed no apparent relationship with the IC₅₀ value of antiprion activity (data not shown), suggesting that the chemicals found here might exert their antiprion action in a manner that differs from those of previously reported antiprion chemicals such as antimalarias and amyloid binding dyes.

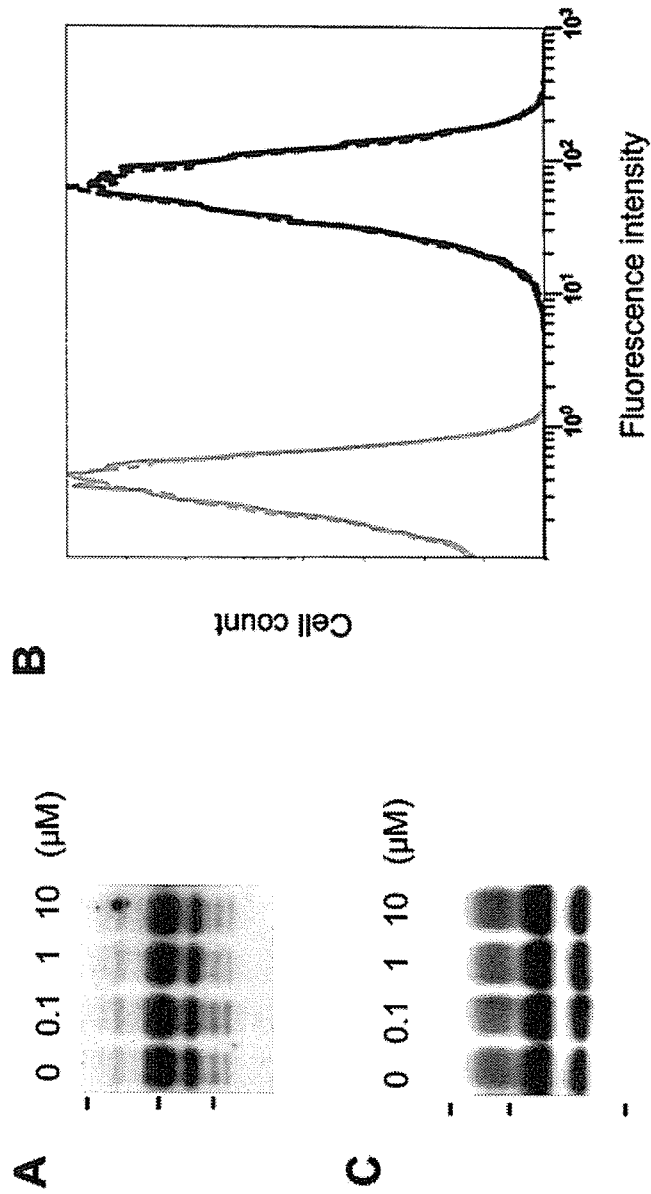


Fig. 1. Effects of a representative chemical, chrysoidine, on the cellular PrP (A, B) and the cell lysate abnormal PrP (C). (A) Immunoblot data of the total cellular PrP in noninfected NB cells treated with a designated dose of chrysoidine. Bars on the *left* indicate molecular size markers at 81, 42, and 32 kDa. (B) Flow cytometry data of the cell surface PrP in noninfected NB cells treated with 1 μ M chrysoidine. *Solid line* and *broken line* indicate chrysoidine-treated cells and nontreated cells, respectively. *Grey line* peaks on the *left* show their respective isotype controls. (C) Immunoblot data of the abnormal PrP from ScNB cell lysate preincubated with a designated dose of chrysoidine prior to protease digestion. Molecular size markers on the left are 42, 32, and 18 kDa.

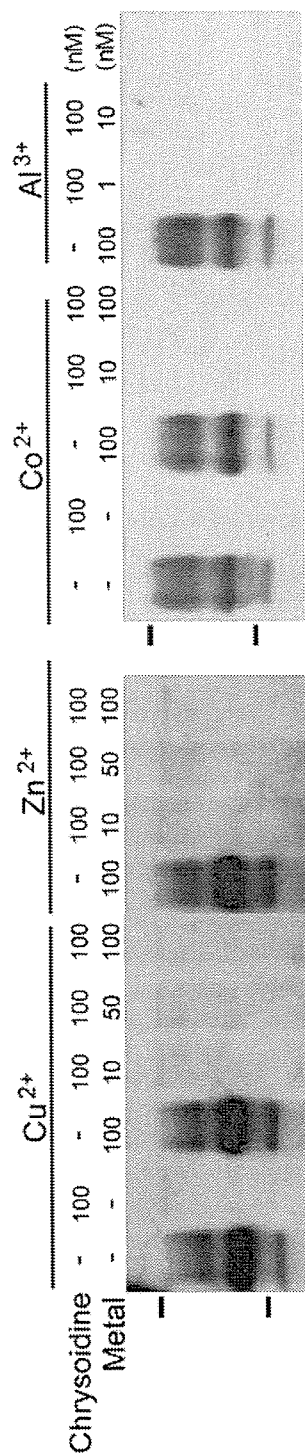


Fig. 2. Antiprion activity in ScNB cells of chrysoidine preincubated with metal ions. Immunoblot data of the abnormal PrP are shown. Bars on the *left* indicate molecular size markers at 37 and 25 kDa.

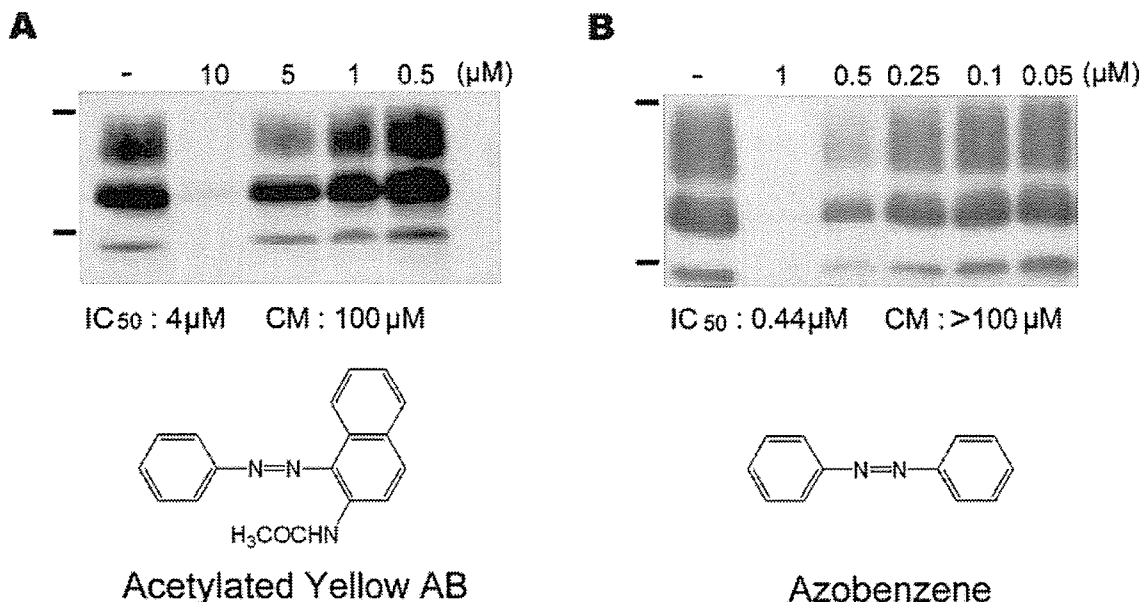


Fig. 3. Antiprion activity in ScNB cells of acetylated Yellow AB (A) and azobenzene (B) Immunoblot data of the abnormal PrP are shown. Bars on the left indicate molecular size markers at 37 and 25 kDa. IC₅₀ is approximate dose giving 50% inhibition of abnormal PrP formation. CM is approximate maximal dose that does not affect the rate of cell growth.

Brain Endothelial Permeability

The brain is the main organ that is affected in prion diseases. Therefore, therapeutic compounds must penetrate into the brain. To examine the permeability of a chemical through the blood–brain barrier, we used a simple analytical model consisting of brain capillary endothelial MBEC4 cells. As a representative of the effective chemicals found in the study, chrysoidine was examined in this model and compared with a paracellular marker, Na-F, as well as a control, quinacrine, which has been used for clinical trials of patients with prion diseases. The results showed that the respective permeability coefficients of Na-F, quinacrine, and chrysoidine were 2.17×10^{-3} , 0.96×10^{-3} , and 4.63×10^{-3} cm/min (Fig. 5). Therefore, chrysoidine penetrated the brain capillary endothelial cells about five times more efficiently than quinacrine.

DISCUSSION

Here, we revealed that chelating chemicals, especially aromatic azo compounds, have antiprion activity. Mechanisms of their antiprion action apparently include neither alteration of cellular PrP level nor direct modification of abnormal PrP. Taken together with previous findings related to the interaction of PrP with metals (review in Brown, 2004), the data obtained through the present study suggest that the chelating activity might influence the antiprion action but is not essential for

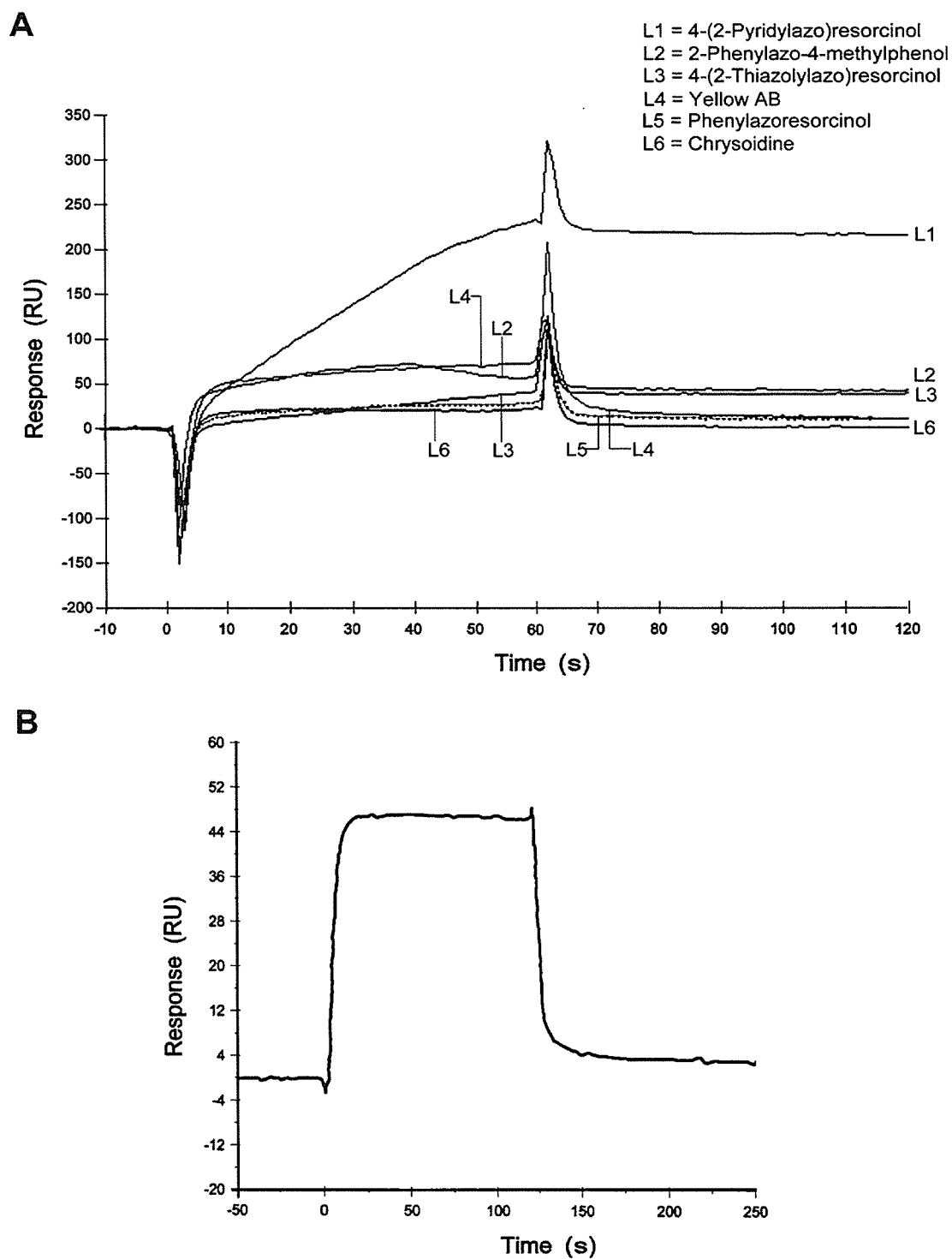


Fig. 4. SPR sensorgrams of chelating compounds (A) and quinacrine (B) interacting with PrP121–231. Each chemical at 50 μ M was analyzed using a *ca.* 3,000 RU PrP-bound biosensor chip. Each phase of association and dissociation was monitored for 60 s in (A) or 125 s in (B).

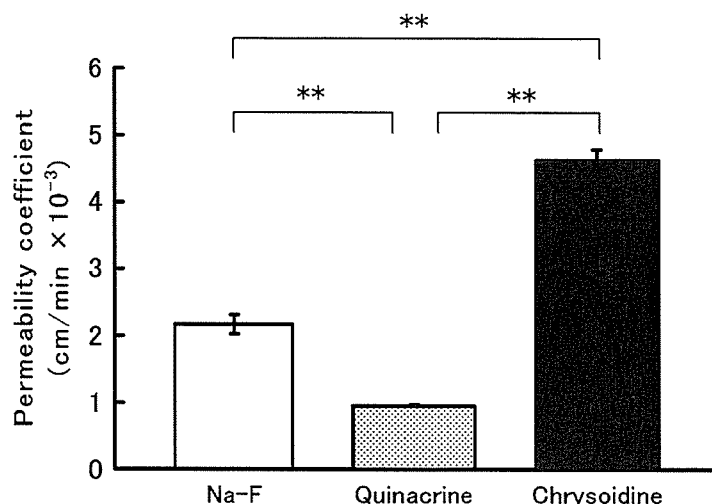


Fig. 5. Permeability coefficients of Na-F, quinacrine, and chrysoidine through MBEC4 monolayer. Each chemical at 100 μ M was analyzed. The values are mean \pm SEM ($n = 3$ –4 inserts). ** $p < 0.01$; significant difference between each group.

it. This inference is consistent with our previous results from quinacrine derivatives carrying chelating activities (Murakami-Kubo *et al.*, 2004).

Chrysoidine, a representative chemical found in this study, is far superior to quinacrine in both the antiprion activity and the brain endothelial permeability. The respective antiprion activities of chrysoidine and quinacrine in ScNB cells were 15 nM and 400 nM in IC_{50} , indicating that chrysoidine is about 27 times more effective than quinacrine. Furthermore, chrysoidine penetrated brain capillary endothelial cells about five times more efficiently than quinacrine. In addition, chrysoidine is much less toxic than quinacrine because a maximal dose at which the ScNB cell growth to confluence is still tolerant was more than 100 μ M in chrysoidine or 2 μ M in quinacrine (Table II). These findings suggest that chrysoidine might be more beneficial *in vivo* than quinacrine, but the *in vivo* efficacy of chrysoidine remains to be evaluated.

Results from the SPR analysis obtained here were not consistent with those of our previous study (Kawatake *et al.*, 2006), where the SPR binding response correlates with the inhibition activity of abnormal PrP formation in ScNB cells. Chrysoidine, the most effective chemical in the study, has a similar structure to either half of a symmetrical compound, Congo red, whose antiprion activity ($IC_{50} = 14$ nM) is as prominent as that of chrysoidine ($IC_{50} = 15$ nM) (Table II) but whose permeability into the brain is reportedly very poor because of low lipophilicity and high charge in its acidic groups (Klunk *et al.*, 2002). Interaction with recombinant PrP121–231 differs greatly between chrysoidine and Congo red. Congo red has very high affinity ($K_D = 1.6$ μ M) and strong binding response (1.7 RU/Da at 10 μ M using a *ca.* 3,000 RU PrP-bound biosensor chip) to the PrP121–231 (Kawatake *et al.*, 2006), whereas chrysoidine shows a sensorgram pattern of low affinity compounds and has very low binding response (0.1 RU/Da at 50 μ M using a similar

biosensor chip). These facts suggest that chrysoidine exerts its antiprion action in a manner that differs from that of Congo red, but this inference demands further evaluation.

The brain endothelial permeability assay using MBEC4 cells revealed that the permeability coefficient of quinacrine was much lower than that of Na-F. The results are consistent with those of our previous experiments (Dohgu *et al.*, 2004). Quinacrine transport through the blood–brain barrier is mediated by both the efflux system (P-glycoproteins) and the influx system (organic cation transporter-like machinery). Therefore, quinacrine entry into the brain is controlled by three factors: P-glycoprotein-mediated active efflux at the apical side of the plasma membrane; highly concentrative uptake system; large storage capacity in the cytoplasm of the brain endothelial cells. On the contrary, Na-F is transported through paracellular routes (tight junctions) at the blood–brain barrier, and neither active efflux nor concentrative uptake system is involved in the Na-F permeability. These differences might explain the reason why quinacrine is less efficiently permeabilized than Na-F.

Chrysoidine is used in various fields as a yellowish fluorescent dye. This chemical was suggested to relate with bladder cancer in humans (Cartwright *et al.*, 1983; Sole and Sorahan, 1985), but it is still controversial because the data of a later conducted case-control study denied its relation to the cancer (Sorahan and Sole, 1990). There are no data on the genetic and related effects of the chemical in humans, but it is mutagenic to bacteria and toxic to rat hepatocytes *in vitro* (Sandhu and Chipman, 1990). In the mice orally administered, it produced liver carcinoma, leukemia, and reticulum cell sarcomas (Anonymous, 1975). These findings suggest that clinical use of chrysoidine or related chemicals might be inadequate.

In conclusion, we screened chelating chemicals and found that chrysoidine was much more effective in both antiprion activity and brain endothelial permeability than quinacrine, and it was much less toxic in NB cells. The mechanism of antiprion action of this compound did not apparently include alteration of cellular PrP level, direct modification of abnormal PrP, or chelation of metals. Its interaction with PrP121–231 differed greatly from that of Congo red, despite their structural similarity. These findings will contribute to the development of therapeutic compounds for prion diseases.

ACKNOWLEDGMENTS

This study was supported by a Grant (H16-kokoro-024) to K.D. from the Ministry of Health, Labor, and Welfare, Japan. The authors thank Drs. Jiro Takata, Atsushi Yamauchi, Shinya Dohgu, Satoshi Kawatake, Toru Iwaki, and Kenta Teruya for their suggestions, and Ms. Kyomi Sasaki for manuscript preparation.

REFERENCES

- Anonymous. (1975). Chrysoidine. *Int. Agency Res. Cancer Monogr.* **8**:91–96.
Brown, D. R. (2004). Metallic prions. *Biochem. Soc. Symp.* **71**:193–202.

- Cartwright, R. A., Robinson, M. R. G., Glashan, R. W., Gray, B. K., Hamilton-Stewart, P., Cartwright, S. C., and Barnham-Hall, D. (1983). Does the use of stained maggots present a risk of bladder cancer to coarse fishermen? *Carcinogenesis* **4**:111–113.
- Dehouck, M. P., Jolliet-Riant, P., Brée, F., Fruchart, J. C., Cecchelli, R., and Tillement, J. P. (1992). Drug transfer across the blood–brain barrier: Correlation between *in vitro* and *in vivo* models. *J. Neurochem.* **58**:1790–1797.
- Dohgu, S., Yamauchi, A., Takata, F., Sawada, Y., Higuchi, S., Naito, M., Tsuruo, T., Shirabe, S., Niwa, M., Katamine, S., and Kataoka, Y. (2004). Uptake and efflux of quinacrine, a candidate for the treatment of prion diseases, at the blood–brain barrier. *Cell. Mol. Neurobiol.* **24**:205–217.
- Doh-Ura, K., Iwaki, T., and Caughey, B. (2000). Lysosomotropic agents and cysteine protease inhibitors inhibit scrapie-associated prion protein accumulation. *J. Virol.* **74**:4894–4897.
- Frostell-Karlsson, A., Remaeus, A., Roos, H., Andersson, K., Borg, P., Hamalainen, M., and Karlsson, R. (2000). Biosensor analysis of the interaction between immobilized human serum albumin and drug compounds for prediction of human serum albumin binding levels. *J. Med. Chem.* **43**:1986–1992.
- Ishikawa, K., Doh-ura, K., Kudo, Y., Nishida, N., Murakami-Kubo, I., Ando, Y., Sawada, T., and Iwaki, T. (2004). Amyloid imaging probes are useful for detection of prion plaques and treatment of transmissible spongiform encephalopathies. *J. Gen. Virol.* **85**:1785–1790.
- Kawatake, S., Nishimura, Y., Sakaguchi, S., Iwaki, T., and Doh-ura, K. (2006). Surface plasmon resonance analysis for the screening of anti-prion compounds. *Biol. Pharm. Bull.* **29**:927–932.
- Kim, C.-L., Karim, A., Ishiguro, N., Shinagawa, M., Sato, M., and Horiuchi, M. (2004). Cell-surface retention of PrPC by anti-PrP antibody prevents protease-resistant PrP formation. *J. Gen. Virol.* **85**:3473–3482.
- Klunk, W. E., Bacskaï, B. J., Mathis, C. A., Kajdasz, S. T., McLellan, M. E., Frosch, M. P., Debnath, M. L., Holt, D. P., Wang, Y., and Hyman, B. T. (2002). Imaging Aβ plaques in living transgenic mice with multiphoton microscopy and methoxy-X04, a systemically administered Congo red derivative. *J. Neuropathol. Exp. Neurol.* **61**:797–805.
- Murakami-Kubo, I., Doh-Ura, K., Ishikawa, K., Kawatake, S., Sasaki, K., Kira, J., Ohta, S., and Iwaki, T. (2004). Quinoline derivatives are therapeutic candidates for transmissible spongiform encephalopathies. *J. Virol.* **78**:1281–1288.
- Nakajima, M., Yamada, T., Kusuhara, T., Furukawa, H., Takahashi, M., Yamauchi, A., and Kataoka, Y. (2004). Results of quinacrine administration to patients with Creutzfeldt–Jakob disease. *Dement. Geriatr. Cogn. Disord.* **17**:158–163.
- Prusiner, S. B. (1991). Molecular biology of prion diseases. *Science* **252**:1515–1522.
- Race, R. E., Caughey, B., Graham, K., Ernst, D., and Chesebro, B. (1988). Analyses of frequency of infection, specific infectivity, and prion protein biosynthesis in scrapie-infected neuroblastoma cell clones. *J. Virol.* **62**:2845–2849.
- Sandhu, P., and Chipman, J. K. (1990). Bacterial mutagenesis and hepatocyte unscheduled DNA synthesis induced by chrysoidine azo-dye components. *Mutat. Res.* **240**:227–236.
- Sole, G., and Sorahan, T. (1985). Coarse fishing and risk of urothelial cancer. *Lancet* **1**:1477–1479.
- Sorahan, T., and Sole, G. (1990). Coarse fishing and urothelial cancer: A regional case-control study. *Br. J. Cancer* **62**:138–141.
- Tatsuta, T., Naito, M., Oh-hara, T., Sugawara, I., and Tsuruo, T. (1992). Functional involvement of P-glycoprotein in blood–brain barrier. *J. Biol. Chem.* **267**:20383–20391.

Inhibition of Transforming Growth Factor- β Production in Brain Pericytes Contributes to Cyclosporin A-Induced Dysfunction of the Blood-Brain Barrier

Fuyuko Takata,^{1,2} Shinya Dohgu,¹ Atsushi Yamauchi,¹ Noriko Sumi,¹ Shinsuke Nakagawa,^{2,3} Mikihiro Naito,⁴ Takashi Tsuruo,⁴ Hideki Shuto,¹ and Yasufumi Kataoka^{1,2,5}

Received July 24, 2006; accepted October 5, 2006

SUMMARY

1. The present study was designed to clarify whether brain pericytes and pericyte-derived transforming growth factor- β 1 (TGF- β 1) participate in cyclosporin A (CsA)-induced dysfunction of the blood-brain barrier (BBB).

2. The presence of brain pericytes markedly aggravated CsA-increased permeability of MBEC4 cells to sodium fluorescein and accumulation of rhodamine 123 in MBEC4 cells.

3. Exposure to CsA significantly decreased the levels of TGF- β 1 mRNA in brain pericytes in pericyte co-cultures. Treatment with TGF- β 1 dose-dependently inhibited CsA-induced hyperpermeability and P-glycoprotein dysfunction of MBEC4 cells in pericyte co-cultures.

4. These findings suggest that an inhibition of brain pericyte-derived TGF- β 1 contributes to the occurrence of CsA-induced dysfunction of the BBB.

KEY WORDS: Cyclosporin A; brain pericytes; transforming growth factor- β ; blood-brain barrier; permeability; P-glycoprotein; mouse brain endothelial cells.

INTRODUCTION

Cyclosporin A (CsA), a cyclic 11-amino acid peptide, is widely used as a potent immunosuppressant to prevent allograft rejection in solid organ transplantation and in fatal graft-versus-host disease after bone marrow transplantation; it is also used to treat various autoimmune diseases including rheumatoid arthritis (Ka-

¹ Department of Pharmaceutical Care and Health Sciences, Faculty of Pharmaceutical Sciences, Fukuoka University, Jonan-ku, Fukuoka, 814-0180, Japan.

² PharmaCo-Cell Company Ltd., Nagayo-machi, Nagasaki, 851-2127, Japan.

³ Department of Pharmacology 1, Nagasaki University School of Medicine, Sakamoto, Nagasaki, 852-8501, Japan.

⁴ Institute of Molecular and Cellular Biosciences, University of Tokyo, Bunkyo-ku, Tokyo, 113-0032, Japan.

⁵ To whom correspondence should be addressed; e-mail: ykataoka@fukuoka-u.ac.jp.

han, 1989). Despite its high efficacy, CsA has adverse effects including nephrotoxicity, cardiovascular disorders, gastrointestinal disorders and neurotoxicity. CsA-associated neurotoxicity occurs with a relatively high frequency (20–40%) in organ-transplanted patients with high blood drug levels or within the therapeutic range (The U.S. Multicenter FK506 Liver Study Group, 1994; Pirsch *et al.*, 1997; Gijtenbeek *et al.*, 1999). However, the mechanism of CsA-induced neurotoxicity remains obscure.

The entry of CsA into the brain is usually prevented by the tight junctions and P-glycoprotein (P-gp), a multi-drug efflux pump, of brain microvascular endothelial cells. But CsA-associated neurotoxicity, including tremors, seizures and encephalopathy, strongly suggests the possibility that CsA is transported across the blood-brain barrier (BBB). We previously reported that CsA produced convulsions by inhibiting γ -aminobutyric acid (GABA)ergic neural activity and the binding properties of the GABA_A receptor (Shuto *et al.*, 1999). The inhibition of GABAergic neurotransmission by CsA may lead to an activation of serotonergic neural activity and, consequently, produce tremors (Shuto *et al.*, 1998). These *in vivo* findings are considered to be due to a direct action of CsA transported across the BBB rather than an indirect effect of CsA in the periphery. Indeed, we previously demonstrated that a high concentration of CsA decreased the function and expression of P-gp in brain capillary endothelial cells (Kochi *et al.*, 1999, 2000). The BBB is primarily formed from these cells, which are closely sealed by tight junctions (Pardridge, 1999). P-gp is abundantly expressed in brain endothelial cells and limits the accumulation of many hydrophobic molecules and toxic substances in the brain (Schinkel, 1999). Brain capillary endothelial cells are surrounded by two other cellular components of the BBB, astrocytes and brain pericytes. We also previously reported that the presence of astrocytes markedly aggravated CsA-induced hyperpermeability of, and P-gp dysfunction in, MBEC4 cells, through the acceleration of NO production (Dohgu *et al.*, 2004a). Brain pericytes are important for the growth and migration of endothelial cells and the integrity of microvascular capillaries (Thomas, 1999; Ramsauer *et al.*, 2002). Brain capillary endothelial cells communicate closely with brain pericytes to maintain the BBB (Hori *et al.*, 2004; Dohgu *et al.*, 2005). Transforming growth factor- β (TGF- β) is a cytokine produced by pericytes (Antonelli-Orlidge *et al.*, 1989). We previously reported that brain pericytes contribute to the up-regulation of barrier function and P-gp activity in brain endothelial cells through production of TGF- β 1 (Dohgu *et al.*, 2005).

The present study was designed to clarify whether brain pericytes and pericyte-derived TGF- β participate in CsA-induced dysfunction of the BBB. We first evaluated the effect of CsA on the permeability of, and P-gp function in, mouse brain capillary endothelial (MBEC4) cells, either alone or co-cultured with human brain pericytes. Next, the effect of CsA on TGF- β 1 mRNA expression in brain pericytes and the effect of TGF- β 1 on CsA-decreased BBB function were examined in a co-culture system containing MBEC4 cells and brain pericytes.

MATERIALS AND METHODS

Materials

CsA was kindly supplied by Novartis Pharma (Basel, Switzerland). Sodium fluorescein (Na-F, MW 376), rhodamine 123 and human TGF- β 1 were purchased from Sigma (St. Louis, MO). Culture medium and subculture reagents were obtained from Invitrogen (Carlsbad, CA). All remaining reagents of analytical grade were purchased from Wako (Osaka, Japan).

Cell Culture

MBEC4 cells, isolated from BALB/c mouse brain cortices and immortalized by SV40-transformation (Tatsuta *et al.*, 1992), were cultured in Dulbecco's modified Eagle's medium (DMEM) supplemented with 10% fetal bovine serum, 100 units/mL penicillin and 100 μ g/mL streptomycin. Human brain pericytes (CS-ABI-499, Cell Systems Corporation, Kirkland, WA) were cultured in CS-C Complete Medium Kit (Cell Systems Corporation). They were grown in a humidified atmosphere of 5% CO₂/95% air at 37°C. To make an *in vitro* BBB model, brain pericytes (20,000 cells/cm²) were first cultured in the wells of a 12-well culture plate. After 2 days, MBEC4 cells (42,000 cells/cm²) were seeded on the inside of the collagen-coated polycarbonate membrane (1.0 cm², 3.0 μ m pore size) of a Transwell®-Clear insert (12-well type, Costar, MA) placed in the plate containing layers of brain pericytes (pericyte co-culture). A monolayer system was also generated with MBEC4 cells alone (MBEC4 monolayer).

Cell viability was assessed using a WST-8 assay (Cell Counting Kit, DOJINDO, Kumamoto, Japan). The absorbance of a highly water-soluble formazan dye (WST-8), reduced by mitochondrial dehydrogenase, was measured in each sample at wavelengths of 450-nm (test wavelength) and 700-nm (reference wavelength).

Treatment with CsA and TGF- β 1

TGF- β 1 was dissolved in 4 mM HCl containing 1 mg/mL of bovine serum albumin; CsA was dissolved in ethanol. Each original solution was then diluted with serum-free medium. The final concentrations in the test media were 4 μ M HCl/1 μ g/mL bovine serum albumin or 0.1% ethanol. MBEC4 cells were cultured for 3 days, and the inserts were washed three times with serum-free medium. Cells were then exposed for 1–12 h to 5 μ M of CsA injected into the inside of the insert (luminal side). Alternatively, TGF- β 1 (0.01–1 ng/mL) was loaded on the luminal side. In parallel, cells were treated with serum-free medium containing the corresponding amount of ethanol and/or HCl and bovine serum albumin as the vehicle.

Transcellular Transport of Na-F

To initiate the transport experiments, the medium was removed and MBEC4 cells were washed three times with Krebs–Ringer buffer (118 mM NaCl, 4.7 mM KCl, 1.3 mM CaCl₂, 1.2 mM MgCl₂, 1.0 mM NaH₂PO₄, 25 mM NaHCO₃, and 11 mM D-glucose, pH 7.4). Krebs–Ringer buffer (1.5 mL) was added to the outside of the insert (abluminal side). Krebs–Ringer buffer (0.5 mL) containing 100 µg/mL of Na-F was loaded on the luminal side of the insert. Samples (0.5 mL) were removed from the abluminal chamber at 10, 20, 30 and 60 min and immediately replaced with fresh Krebs–Ringer buffer. Aliquots (5 µL) of the abluminal medium were mixed with 200 µL of Krebs–Ringer buffer and the concentration of Na-F was determined using a fluorescence multiwell plate reader (Ex(λ) 485 nm; Em(λ) 530 nm) (CytoFluor Series 4000, PerSeptive Biosystems, Framingham, MA). The permeability coefficient and clearance were calculated according to the method described by Dehouck *et al.* (1992). Clearance was expressed as microliters (µL) of tracer diffusing from the luminal to abluminal chamber and was calculated from the initial concentration of tracer in the luminal chamber and final concentration in the abluminal chamber: clearance (µL) = $[C]_A \times V_A / [C]_L$ where $[C]_L$ is the initial luminal tracer concentration, $[C]_A$ is the abluminal tracer concentration and V_A is the volume of the abluminal chamber. During the 60-min period of the experiment, the clearance volume increased linearly with time. The average volume cleared was plotted against time, and the slope was estimated by linear regression analysis. The slope of clearance curves for the MBEC4 monolayer or co-culture systems was denoted by PS_{app} , where PS is the permeability–surface area product (in µL/min). The slope of the clearance curve with a control membrane was denoted by $PS_{membrane}$. The real PS value for the MBEC4 monolayer and the co-culture system (PS_{trans}) was calculated as $1/PS_{app} = 1/PS_{membrane} + 1/PS_{trans}$. The PS_{trans} values were divided by the surface area of the Transwell inserts to generate the permeability coefficient (P_{trans} , in cm/min).

Functional Activity of P-gp

The functional activity of P-gp was determined by measuring the cellular accumulation of rhodamine 123 (Sigma) according to the method of Fontaine *et al.* (1996). MBEC4 cells were washed three times with assay buffer (143 mM NaCl, 4.7 mM KCl, 1.3 mM CaCl₂, 1.2 mM MgCl₂, 1.0 mM NaH₂PO₄, 10 mM HEPES, and 11 mM D-glucose, pH 7.4), and then incubated in 0.5 mL of assay buffer containing 5 µM rhodamine 123 for 60 min. The solution was then removed and the cells were washed three times with ice-cold phosphate-buffered saline and solubilized in 1 M NaOH (0.2 mL). The solution was neutralized with 1 M HCl (0.2 mL) and the rhodamine 123 content was determined using a fluorescence multiwell plate reader (Ex(λ) 485 nm; Em(λ) 530 nm, CytoFluor Series 4000). Protein concentration was measured by the method of Bradford (Bradford, 1976).

Expression of TGF- β 1 Receptor mRNA in MBEC4 Cells and Human Brain Pericytes

Reverse-transcription polymerase chain reaction (RT-PCR) was employed to determine the level of mRNA expression for TGF- β 1 receptor I and II in MBEC4 cells and brain pericytes. Total RNA was extracted from cultured cells using TRIzolTM reagent (Invitrogen, Carlsbad, CA) and 1 μ g of RNA was reverse-transcribed and amplified by PCR using a SuperScript One-Step RT-PCR system (Invitrogen). Amplification was performed in a DNA thermal cycler (PC707; ASTEC, Fukuoka, Japan). The primers used and PCR conditions are summarized in Table I. Ten microliters of each PCR product was analyzed by electrophoresis on a 2% agarose (Sigma) gel with ethidium bromide staining. Gels were visualized on a UV light transilluminator and photographed using a DC290 Zoom digital camera (Kodak, Rochester, New York).

Relative Quantitation of TGF- β 1 mRNA by Real-Time RT-PCR

Real-time RT-PCR was employed to determine the level of TGF- β 1 gene expression in brain pericytes with CsA-treated pericyte co-culture. Total RNA was extracted from brain pericytes using TRIzolTM reagent (Invitrogen) and 2 μ g RNA was reverse-transcribed using a SuperScriptTM III First-Strand Synthesis System (Invitrogen) in a total volume of 20 μ L, according to the manufacturer's protocol.

Real-time PCR was conducted on an Mx3000PTM Multiplex Quantitative PCR System (Stratagene, La Jolla, CA) with 2 μ L of reverse-transcription product, BrilliantTM SYBR[®] Green QPCR Master Mix (Stratagene), primers at 150 nM and reference dye, in a total volume of 50 μ L as per the manufacturer's protocol. The following PCR conditions were employed: 95°C for 10 min, followed by cycles of 95°C for 30 s, 54°C for 60 s and 72°C for 90 s. The sequences of primers were as follows: sense primer 5'-CCCTGGACACCAACTATTG-3' and antisense primer 5'-CCGGGTTATGCTGGTTGTA-3' for TGF- β 1 (Untergasser *et al.*, 2005); sense primer 5'-GAGTCAACGGATTGTCGT-3' and antisense primer 5'-TTGATTTTGGAGGGATCTCG-3' for glyceraldehyde-3-phosphate dehydrogenase (GAPDH; GenBank Accession Number, M33197). After amplification, a melting curve was obtained by heating at 55°C and fluorescence data were collected at 0.2°C/s.

Relative quantitative analysis was performed employing Mx3000PTM Multiplex Quantitative PCR System software (Stratagene). We used the expression of GAPDH to normalize the expression data for the TGF- β 1 gene. For a comparative analysis, values from vehicle treated brain pericytes were arbitrarily set as 1. Each sample was analyzed in triplicate.

Statistical Analysis

Values are expressed as means \pm SEM. Statistical analysis was performed using Student's *t*-test. One-way and two-way analyses of variance (ANOVAs) followed by Tukey-Kramer's tests or Dunnett tests were applied to multiple com-